Multifunctional ZnCuNiAgO composites synthesized by green method: enhanced optical and antibacterial activities

S. Shanmugapriya[1], and A. Rajendiran[1]*

[1]Department of Zoology, A. A. Government Arts College, Musiri, Tiruchirappalli, Tamil Nadu-621 211, India.

Abstract

The ZnCuNiAgO composites were synthesized through green method using *Chaetomorpha antennina* seaweed extract. From the XRD patterns of biosynthesized ZnCuNiAgO composites exhibited mixed hexagonal/monoclinic/cubic structure. FESEM image shows that synthesized ZnCuNiAgO composites was formed rack like structure. From the FT-IR spectra, the M-O stretching bands observed at 574 and 465 cm^{-1}forZnCuNiAgO composites. Optical studies was determined by UV-Visible and PL spectra. In order to explore new strategies to identify and develop the next generation of drugs or agents to control a bacterial infection, the antibacterial properties of the ZnCuNiAgO composites was examined by Gram positive and Gram negative strains.

Keywords: Composites; antibacterial activity; XRD; UV; PL; ZnCuNiAgO.

Introduction

Nanocomposite have potentially interest with various applications such as optoelectronic, Photocatalytic and biomedical applications prompted by quantum-size effect. These nanocomposites can be a different of combination such as dielectric/dielectric, dielectric/metal, dielectric/semiconductor, semiconductor/semiconductor etc. Metal oxide nanocomposites are highly stable and essentially used in biocides and disinfectants and this may be long duration than organic-based materials [1, 2].

Marine organism is a novel approach to characterize the variety of compounds with pharmacological activities and nanomedicine applications as potential sources for future drugs. Seaweeds are used as most valuable bioactive compounds in Pharmaceutical, Nutraceutical and Biomedicine industries. In recent years, young researchers carry on their novel approach to synthesize nanocomposite materials against seaweed extract for anti-microbial, anticancer, antifungal and anti-inflammatory activities [3]. The nanoparticles are a

big challenge for new material creation on all types of research aspects. So, eco and phyto-friendly approaches may negotiate the toxic effect of chemical originated silver nanoparticles. Seaweed reported their silver nanomaterials application in medicine to reduce the human diseases [4]. Seaweeds are important source of protein, iodine vitamins, minerals, with their metabolites showing wide range of promising biological activities.*Chaetomorpha antennina* seaweed one of the important marine resource material: which is used for different medical application such as antimicrobial, antioxidant, antiviral and anticancer properties etc [5].

In this investigation, the ZnCuNiAgO compositeshas been synthesized by green method using were *Chaetomorpha antennina* seaweed extract. The structural, morphological, optical, and antibacterial activities were elucidated.

2 Experimental methods

2.1 Synthesis of ZnCuNiAgO composites

The fresh *Chaetomorpha antennina* seaweed was collected from mandapam Rameshwaram, Tamil Nadu, India. The seaweed extracts were prepared by 10 g wet seaweed in 100 mL of double distilled water boiled at 60 °C for few min and extract were filtered by using Whatmann No. 1 filter paper. Zinc nitrate salt, nickel nitrate salt, copper nitrate and silver nitrate salt were used as source materials without further purification.

However, 0.01M of Zn $(NO_3)_2.6H_2O$, 0.01M Cu $(NO_3)_2.6H_2O$, 0.01M Ni $(NO_3)_2.6H_2O$ and 0.01M Ag (NO_3) source materials were dissolved in 50 ml double distilled water. 50 ml of *chaetomorpha antennina*seaweed extract added to 50 mL of aqueous Zinc, copper, nickel nitrate and silver nitrate solution. This mixture solution could be stirred constantly at 80 °C for 5 h. brown precipitates were formed on continuous stirring and nanocomposites was heated at 120 ˚C. Thus, ZnCuNiAgO samples were obtained. Further, the nanocomposites were annealed at 800 °C for 5h. The graphic representation of ZnCuNiAgO prepared by *Chaetomorpha antennina* seaweed extract is represented in fig 1.

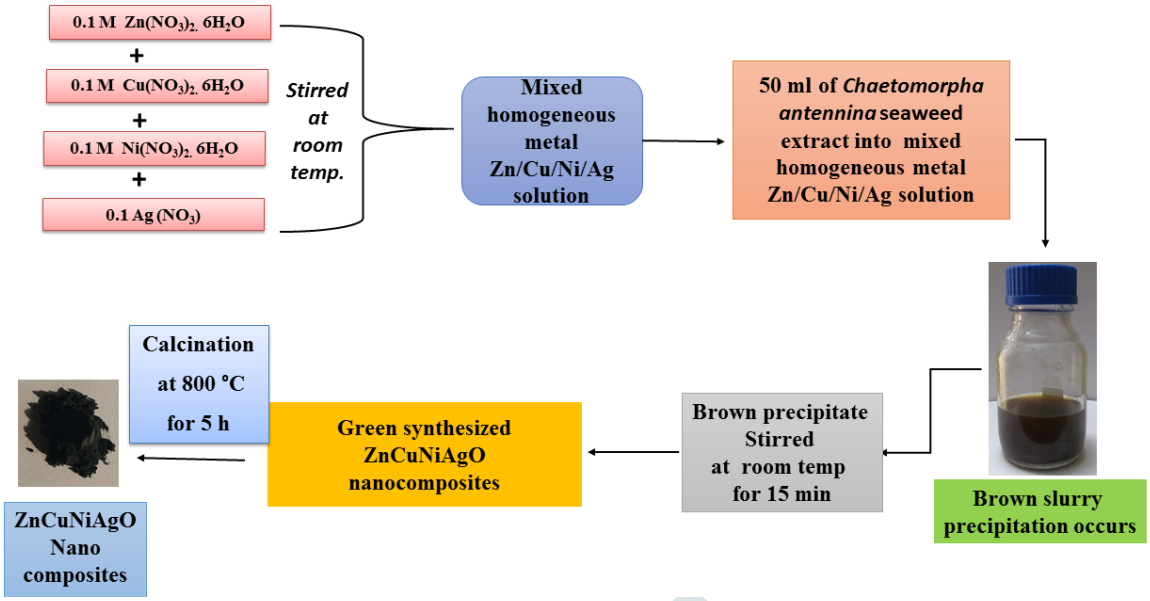

Figure 1 The graphic representation of ZnCuNiAgO prepared by *Chaetomorpha antennina* seaweed extract.

2.2 Antibacterial studies

The antibacterial activity were investigated by the well diffusion method tested against both G+ *(S. pneumonia* and *B. subtilis)* and G- (*E. coli, S. dysenteria, K. pneumonia, V. cholera, P. aeruginosa,* and *P. vulgaris*) bacterial strain treated with ZnCuNiAgO nanocomposites. The well-prepared on a nutrient agar (NA) media plate using gel puncture and the bacterial culture were swabbed on NA media using sterile cotton. After inoculation, testing samples loaded with 2 and 2.5 mg/ml on the bacteria plates and incubated at 37 ˚C for 24 h. The standard antibiotic amoxicillin was used as the positive controls.

2.3 Characterization Techniques

The powered XRD patterns studies was carried out using (model: X'PERT PRO PANalytical) and recorded in the range of 20^{o}-80^{o} for ZnCuNiAgOnanocompositesusing the source as Cu Kα (1.54 Å) radiation. To determine the oxidation state by using XPS spectra (Carl Zeiss). The morphology analysis was carried out by FESEM (Carl Zeiss Ultra 55) with EDX (Inca). The functional groups were identified by FT-IR spectra using (Perkin-Elmer). The optical studies were carried out using Lambda 35 spectrophotometer (UV-VIS) and Cary Eclipse spectrometer (PL).

3. Results and discussion

3.1 X-ray diffraction (XRD) studies

The XRD patterns of biosynthesized ZnCuNiAgO nanocomposites is shown in Fig. 2(a-c). The XRD peaks observed angle at 22.1146, 25.5771, 28.5359, 31.5296, 34.0355, 35.5311, 36.2788, 36.8585, 38.1395,

38.8492, 42.8138, 44.2914, 47.5699, 48.9560, 62.1589, 64.4278, 65.7927 and 74.5327 respectively, and planes are well matched with standard references corresponding to the unit cell of the wurtzite hexagonal structure for ZnO NPs (JCPDS card no: 36-1451), monoclinic structure for CuONPs (JCPDS card no: 45-0937) and face centered cubic structure for NiO NPs (JCPDS 44-1159), respectively. Average crystallite size NPs can be calculated using Debey-scherrar's formula $D = \frac{k\lambda}{\beta cos\theta}$. The average crystallite size is 24 nm for ZnCuNiAgO nanocomposites.

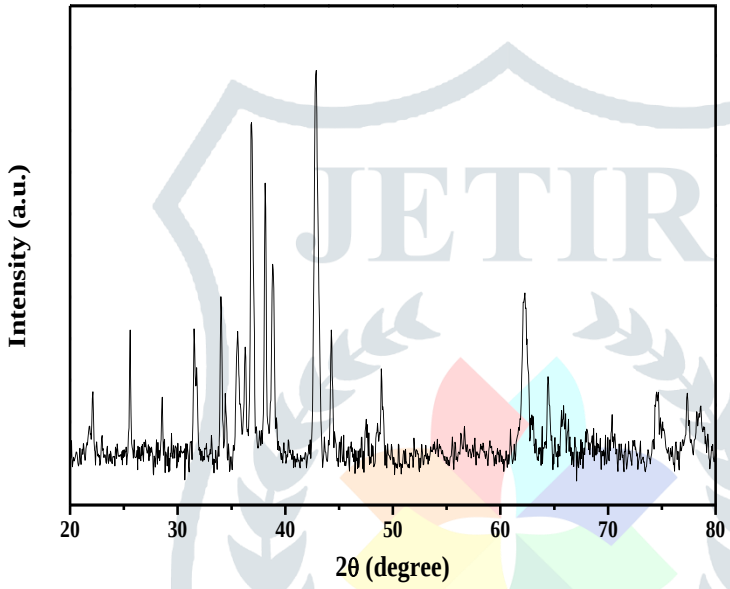

Figure 2 X-ray diffraction patterns of ZnCuNiAgO nanocomposites

3.2 Field emission scanning electron microscopic studies

The surface topography of ZnCuNiAgO nanocomposites using *Chaetomorpha antennina* seaweed extract is shown in Fig. 3(a-b). In the case of FESEM image, the synthesized ZnCuNiAgO nanocomposites formed rack like structure and the particle size is present in the nanoscale level.

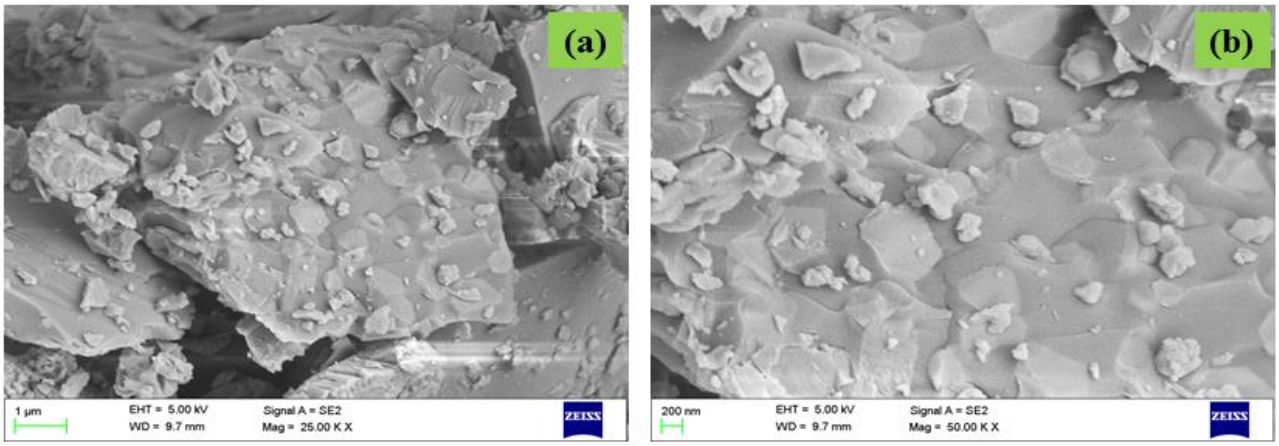

Figure 3 (a-b) FESEM image of low and high magnification of ZnCuNiAgO nanocomposites

3.3 FTIR analysis

The various functional groups of the bio-synthesized ZnCuNiAgO nanocomposites is shown in Fig. 4. The 3399 cm^{-1} (O-H) hydroxyl stretching, 2864 cm^{-1} and 2926 cm^{-1} (C-H) symmetric and asymmetric stretching [6], 1645 cm^{-1} (H-O-H) bending vibration [7],The Metal-oxygen (M-O) peaks appearing between 400 and 600 cm^{-1} [8]. The Zn-Ni-Cu-Ag-O stretching bands observed at574 and 465 cm^{-1} [9] for ZnCuNiAgO nanocomposites.

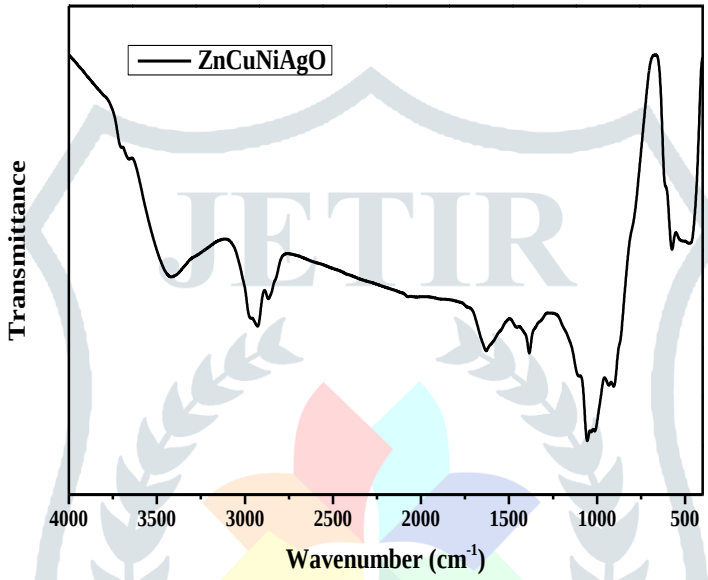

Figure 4 FTIR spectra of ZnCuNiAgO nanocomposites.

3.4 UV-Vis spectroscopic studies

Figure 5 shows the UV-Vis absorbance spectra of green synthesized ZnCuNiAgO composites. The absorption edge are observed around 350-700 nm. The excitonic pecks are observed around 440 nm for ZnCuNiAgO composites. This may be photo-excitation of electron from the valence band to conduction band. The relation between the absorption coefficients α and the incident photon energy hυ can be written as

$$\alpha h\upsilon = A(h\upsilon - E_g)^n$$

Where E_g is the optical bandgap, A is the constant and the exponent n depends on the type of transition. The n = 1/2 for allowed direct transition, 2 for allowed indirect transition 3/2 and 3 for forbidden direct and indirect transitions respectively. Considering direct band transition in without ZnCuNiAgO composites, a plot between $(\alpha h\upsilon)^2$ vs. photon energy hυ and extrapolating the linear portion of the absorption edge to find the intercept with energy axis is shown in Fig. 6.In literature, the ZnO, CuO and NiO NPs band

gap(E_g) are observed at 3.37 eV,1.2 to 2.16 eV and 3.6 eV respectively [10-12]. The calculated band gap of 3.9 eV is obtained for ZnCuNiAgO composites. Therefore, bandgap is tuning the volume fractions of the suitable for several applications such as photovoltaics, photocatalysis and thermoelectrics.

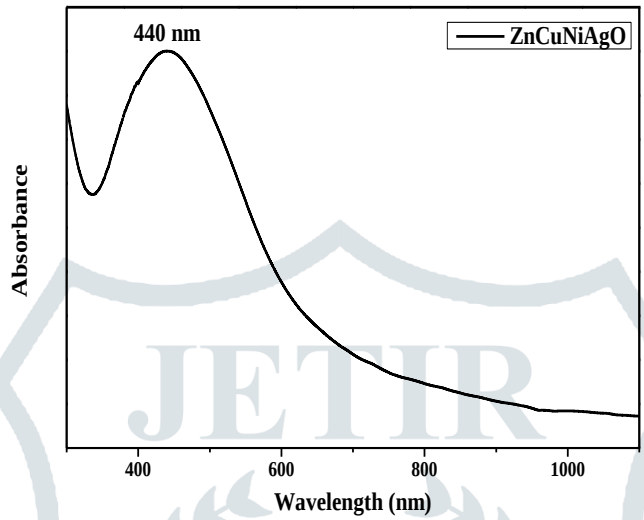

Figure 5 Absorbance spectrum of ZnCuNiAgO composites

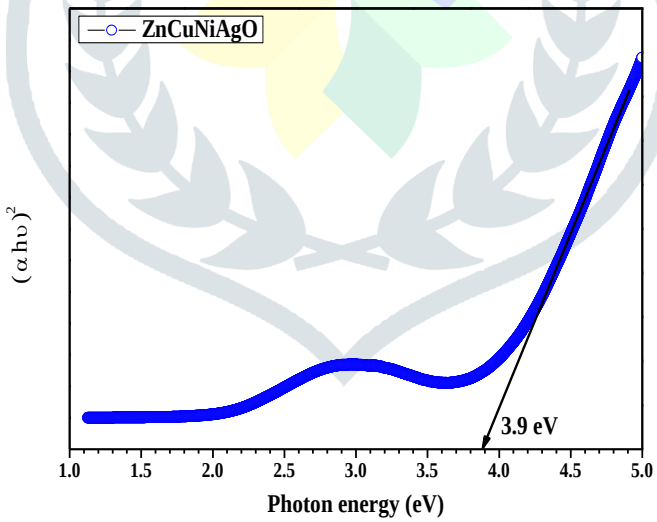

Figure 6 Band gap of ZnCuNiAgO composites.

3.5 Photoluminscence spectroscopic analysis

Figure 7 shows the photoluminescence spectra of biosynthesized ZnCuNiAgO composites using an excitation wavelength of 310 nm. In the case of ZnCuNiAgO composites, the emission wavelengths are observed at 337nm, 371nm, 394nm, 419 nm, 453 nm and 487 nm respectively.The UV emission peaks are observed at337, 371, 394nm, which correspond to radiative recombination of the free exciton-exciton

collision process [13]. In case of visible region, the violet emission (419 nm), blue emission (453 nm) and blue-green emission (489 nm) are ascribed to an oxygen vacancies or Zn, Cu and Ni interstitials. In general, Metal oxide exhibits three types of charge states of oxygen vacancies, such as namely neutral oxygen vacancy (V_o^o), singly ionized oxygen vacancy (V_o^+) and doubly ionized oxygen vacancy (V^{o++})[14-16].

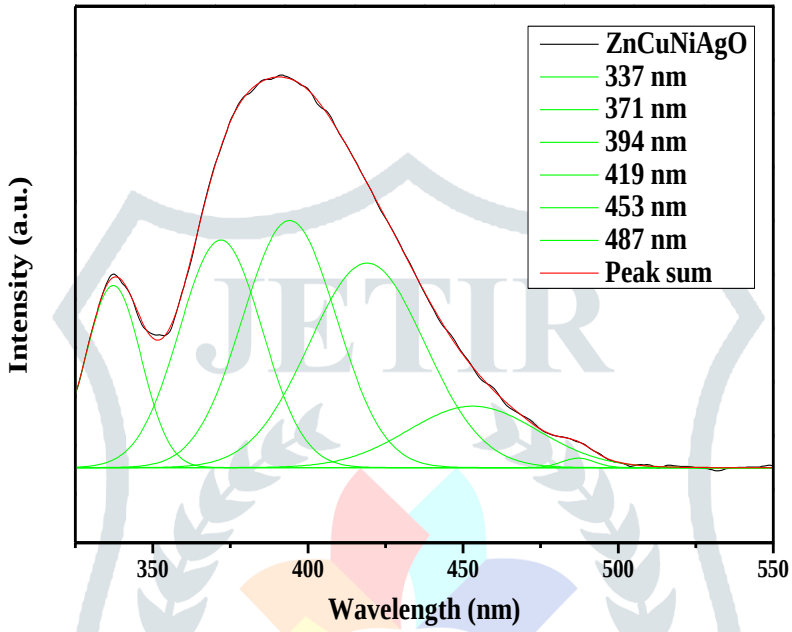

Figure 7 PL spectrum of ZnCuNiAgO composites.

3.6 Antibacterial activity

The antibacterial activity studies were carried out ZnCuNiAgO compositesand evaluated against the set of G+ bacterial strains (*S. pneumoniae and B. subtilis*) and G- bacterial strains (*E. coli, S.dysenteria, K. pneumonia, V. cholera, P. aeruginosa, and P. vulgaris*) (Fig. 8 and Fig. 9). Biosynthesized ZnCuNiAgO composites exhibited antibacterial effect. The antibacterial activity generally determined the presence of Reactive oxygen species (ROS). The metal oxide NPs are produce ROS, due to various effects such as small particle size, oxygen vacancies, and release of $Zn^{2+}/Ni^{2+}/Cu^{2+}/Ag^{3+}$. In the early literature, the higher antibacterial activity result was observed at smaller particles size more antibacterial effects. From the XRD results shows that average particles size estimated 24 nanometer on behalf of ZnCuNiAgO composites, due to this effect nanocomposites can easily perpetrate into bacterial cell membranes, losing the viability, finally bacterial cells are death.

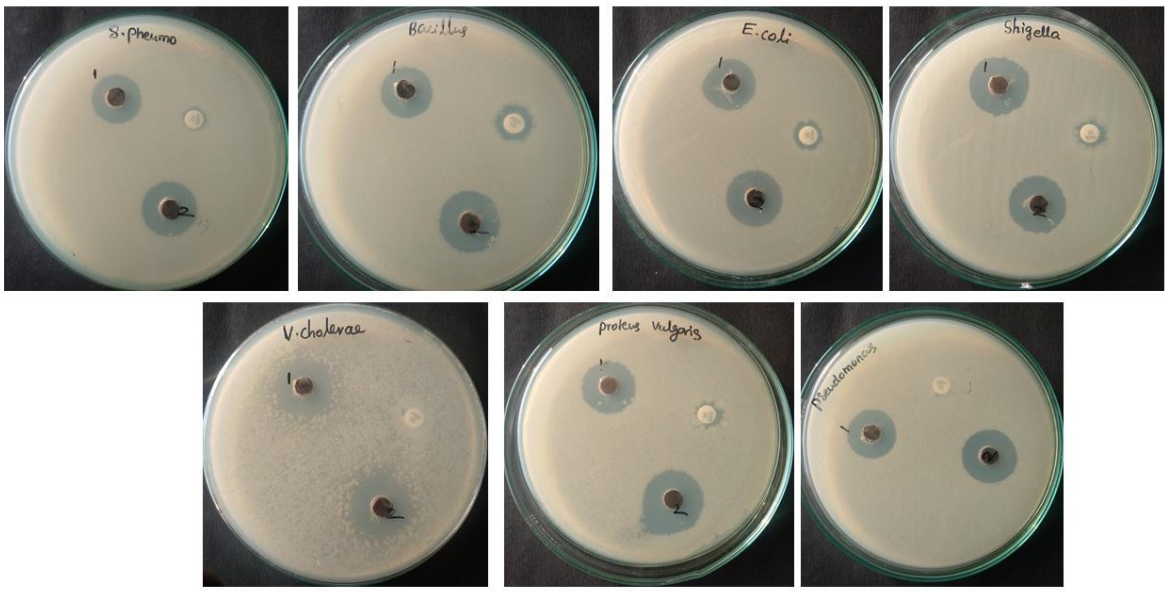

Figure 8 progressive antibacterial activity of ZnCuNiAgO composites

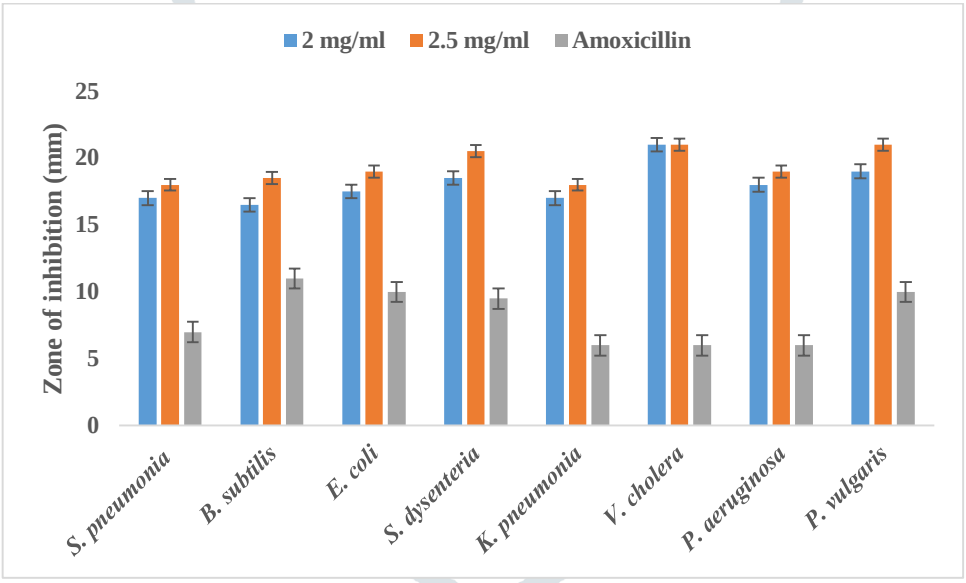

Figure 9The size of the zone of inhibition formed around each well, loaded with test samples, indicating the antibacterial activity towards *G+ and*G- bacterial strains for ZnCuNiAgO composites using *Chaetomorpha antennina* seaweed extract.

Conclusions

In the summery, the ZnCuNiAgO composites was synthesized through green method using *Chaetomorpha antennina* seaweed extract. X-ray diffraction pattern indicates that the green synthesized ZnCuNiAgO composites exhibited mixed wurtzite hexagonal/monoclinic/ cubic structure. FESEM image shows that, the biosynthesized ZnCuNiAgO composites formed rack like structure.In the FTIR spectra, Zn-Ni-Cu-Ag-O stretching bands observed at 574 and 465 cm^{-1} for ZnCuNiAgO composites. The optical band

gaps was found to be3.9 eV for ZnCuNiAgO composites. In the PL emission spectra, various or Zn interstitials, Cu interstitials Ni, oxygen vacanciesand surface defects were observed. The antibacterial activity studies were carried out ZnCuNiAgO composites and evaluated against the set of G+ bacterial strains (*S. pneumoniae and B. subtilis*) and G- bacterial strains (*E. coli, S.dysenteria, K. pneumonia, V. cholera, P. aeruginosa, and P. vulgaris*).

Acknowledgement

One of the author SSP is grateful to the DST-inspire New Delhi, India for sanctioning the financial assistance (IF140182)

References

[1] Karthik, K., S. Dhanuskodi, C. Gobinath, S. Prabukumar, and S. Sivaramakrishnan. "Multifunctional properties of microwave assisted CdO–NiO–ZnO mixed metal oxide nanocomposite: enhanced photocatalytic and antibacterial activities." *Journal of Materials Science: Materials in Electronics* 29, no. 7 (2018): 5459-5471.

[2] R. Joyce Stella, G. Thirumala Rao, B. Babu, V. PushpaManjari,Ch..V. Reddy, J. Shim, R. V. S. S. N. Ravikumar, A facial synthesis and spectral characterization of Cu2+doped CdO/ZnSnanocomposite. J. Magn. Magn. Mater **384**, 6 (2014).

[3] Devi, J. S., Bhimba, B. V., &Ratnam, K. (2012). In vitro anticancer activity of silver nanoparticles synthesized using the extract of Gelidiella sp. *Int J Pharm PharmSci*, *4*(4), 710-15

[4] El Kassas, H. Y., &Attia, A. A. (2014). Bactericidal application and cytotoxic activity of biosynthesized silver nanoparticles with an extract of the red seaweed Pterocladiellacapillacea on the HepG2 cell line. *Asian Pac J Cancer Prev*, *15*(3), 1299-306.

[5] Sapna, M., Swati, R., Anil, K., Meena, V., 2011. Medicinal attributes of Acacia nilotica Linn, a comprehensive review on ethno pharmacological claims. Int. J. Pharm. Life Sci. 2 (6), 830–837.

[6] Zandi, S., P. Kameli, H. Salamati, H. Ahmadvand, and M. Hakimi. "Microstructure and optical properties of ZnO nanoparticles prepared by a simple method." Physica B: Condensed Matter 406, no. 17 (2011): 3215-3218.

[7] Munoz-Hernández, Gerardo, Alejandro Escobedo-Morales, and Umapada Pal. "Thermolytic growth of ZnO nanocrystals: morphology control and optical properties." Crystal Growth and Design 9, no. 1 (2008): 297-300..

[8] Dutta, M., S. Mridha, and D. Basak. "Effect of sol concentration on the properties of ZnO thin films prepared by sol–gel technique." Applied Surface Science 254, no. 9 (2008): 2743-2747.

[9]Xiong, Gang, U. Pal, J. G. Serrano, K. B. Ucer, and R. T. Williams. "Photoluminesence and FTIR study of ZnO nanoparticles: the impurity and defect perspective." physica status solidi c 3, no. 10 (2006): 3577-3581.

[10] Rehman, S., Mumtaz, A., Hasanain, SK, 2011. Size effects on the magnetic and optical properties of CuO nanoparticles. J. Nano. Research. 13(6), 2497-507.

[11]Zheng, H., Ou, JZ.,Strano, MS., Kaner, RB., Mitchell, A., Kalantar-zadeh, K., 2011. Nanostructured tungsten oxide–properties, synthesis, and applications. Adv. Fun. Mater. 21(12):2175-96.

[12] Yoffe, AD., 1993. Low-dimensional systems: quantum size effects and electronic properties of semiconductor microcrystallites (zero-dimensional systems) and some quasi-two-dimensional systems. Adv. in Phys. 42(2),73-262.

[13] X. M. Fan, J. S. Lian, L. Zhao and Y. Liu, *Appl. Sur. Sci.*, 2005, **252,** 420-424.

[14] N. Varghese, L. S. Panchakarla, M. Hanapi, A. Govindaraj and C. N. R. Rao, *Mater. Res. Bull.*, 2007, **42,** 2117-2124.

[15] N. Kumar, A. Dorfman and J. Hahm, *J. Nanosci. Nanotech.*, 2005, **5,** 1915-1918.

[16] D. M. Bagnall, X. F. Chen, M. Y. Shen, Z. Zhu, T. Goto and T. Yao, *J. Cryst. Growth.*,1998, **184,** 605-609.